

# **RESULTS OF THE 2008 UT MODELING BENCHMARK OBTAINED WITH 2 SEMI-ANALYTICAL MODELS: RESPONSES OF FLAT BOTTOM HOLES AT VARIOUS DEPTHS UNDER INTERFACES OF DIFFERENT CURVATURES.**

R. Raillon<sup>1</sup>, S. Mahaut<sup>1</sup>, N. Leymarie<sup>1</sup>, S. Lonne<sup>1</sup> and M. Spies<sup>2</sup>

<sup>1</sup> CEA, LIST, Centre de Saclay, point courrier 120, F-91191 Gif-sur-Yvette cedex, France

<sup>2</sup> Fraunhofer Institute for Techno- & Economy Mathematics ITWM, 67663 Kaiserslautern, Germany

**ABSTRACT.** This paper presents the results of the 2008 UT modeling benchmark with the ultrasonic simulation code for predicting echo-responses from flaws integrated into the Civa software platform and with the code developed by M. Spies. UT configurations addressed are similar to 2007 ones, to better understand some responses obtained last year. Experimental results proposed concern the responses of flat bottom holes at different depths inside surface curved blocks inspected by an immersion probe in normal incidence. They investigate the influence of surface curvature upon the amplitude and shape of flaw responses. Comparison of the simulated and experimental results is discussed.

**Keywords:** Ultrasonic Benchmark, UT Simulation, Semi-Analytical Model, Curvature Study.

**PACS:** 43.35.Yb

## **INTRODUCTION**

The Center for NDE at Iowa State University proposes for the annual benchmark study to re-examine the 2007 benchmark problem where experimental and simulated results of FBH at various depths insonified by normally incident compression waves propagating through interfaces of five different curvatures were compared. The characteristics of the probe used last year (radius, focal length) were questioned [1] and the measurements were made with another probe, very accurately characterized, this year.

Computations of this paper were performed using a model called GPSS (Generalized Point Source Superposition) employed at Fraunhofer ITWM and using the CIVA software, a platform for NDT developed at CEA LIST (French Atomic Energy Commission) [2]. These models for field and echo computations and the benchmark configurations will be briefly described. Then we will present the results of the benchmark studies obtained with the two different codes.

## **BRIEF DESCRIPTION OF THE SIMULATION CODES**

### **GPSS Model for Transducer Beam Representation and Flaw Scattering**

To predict the time-domain signal for the considered problems, the various physical processes involved have to be modeled, which are (i) the radiation of ultrasonic waves by circular, flat or focused transducers and the propagation through the respective medium, (ii)

the reflection and refraction process at the water - aluminum interface, and (iii) the scattering of the waves incident on the model defects SDH and FBH. To account for these processes, a point source superposition technique has been established assuming that the transducer is acting as a piston source. The method is briefly summarized in [3], while a detailed description can be found in [4]. In modeling the transient signals the harmonic (continuous wave) solutions at many frequencies are calculated and then numerically Fourier transformed into the time domain, assuming a respective frequency spectrum function for the transducer input signal of the probe.

To model the reflection and refraction process at the water-aluminum interface, the continuity of the normal tractions and the displacements is used to calculate the particle displacement distribution on the aluminum surface. This distribution is then applied to determine the propagation of the ultrasonic waves into the aluminum block. Finally, the resulting displacement on the defect is calculated using Kirchhoff's theory as described in [5] for the case of anisotropic media. In the calculations, equidistant distributions of grid points within the transducing, refracting and scattering surfaces or interfaces, respectively, are used in accordance with the sampling-theorem. The time-domain signal detected by the transducer is finally determined using Auld's reciprocity theorem for traction-free scatterers: it exploits the displacement and traction at the scatterer's position in presence and absence of the scatterer, respectively [6], in frequency domain, the time-domain signal is then obtained using subsequent inverse Fourier-transformation.

### **CIVA Ultrasonic Models**

Transducer beam model [7]: To calculate the transient wave field radiated inside the specimen, the transducer is discretized as a series of source points over its surface. For each point source, elementary contributions are obtained by means of the pencil method (a high frequency approximation) [8]. The pencil-matrix formulation allows one to predict wavefront radii of curvature along each wave path as well as its time-of-flight; it is combined with the computation of plane wave transmission/reflection coefficients corresponding to each interaction of the pencil with an interface. Impulse responses are then synthesized from these contributions and convolved with the input signal.

Flaw scattering model [9]: The flaw scattering model is based on three steps: calculation of the incident field over the flaw surface, calculation of the flaw scattering using Kirchhoff's approximation, and calculation of the received signal using the reciprocity principle to avoid the integration over the probe in reception. Other models can be used in CIVA like models based on the GTD (Geometrical Theory of Diffraction) for TOFD examination [10]. In this paper, the only model used was that developed under Kirchhoff's approximation.

In echo predictions, the flaw is meshed and the field scattered at each discrete element is obtained from the field incident on this element by applying Kirchhoff's diffraction coefficient (which depends on incident and observation angles for this element and on the polarity of both the incident and the scattered modes). Then, the total scattered field is computed by summing the contributions from all elements. Finally, the reciprocity principle is used to obtain the output signal of the probe acting as a receiver.

### **DESCRIPTION OF THE 2008 ULTRASONIC BENCHMARK**

For a complete description of the configurations studied, see [11].

- **First study:** for the study of surface curvature effect (Figure 1), experiment measurements were made at CEA LIST and it was proposed to simulate the corresponding cases and then compare measured and simulated amplitudes of the echoes. It was also proposed to compare some echoes waveform from 4 FBH chosen because they allow one to observe a shift in phase of the echoes at a given depth. The echoes from 7 flat-bottom holes (0.8 mm diameter), differing by their depths in 5 blocks of different surface curvature radii (two concave, one planar and two convex surfaces) were measured; The probe was different from the one used for the 2007 benchmark: it was a spherically focused probe provided by the Center for NDE, Iowa State University which very accurately characterized it. The CEA LIST characterized it again in the condition of the benchmark measurements. It was used at normal incidence. The nominal diameter is 12.7 mm, the effective geometrical focal length is 6.807 inches (172.9 mm), the center frequency is 4.8 MHz and the -6 dB bandwidth is 88% (of center frequency).

- **Second study:** a side-drilled hole (SDH) longitudinal wave response study was also proposed (Figure 2). The response of side-drilled holes at various depths in a steel block were obtained with the same focused transducer used in the flat-bottom hole study. The water path length, « d », was again 75 mm, and the transducer was oriented to produce 0° refracted P waves in the block. This study was also useful to check the pertinence of the probe parameters used for the simulations in the FBH study.

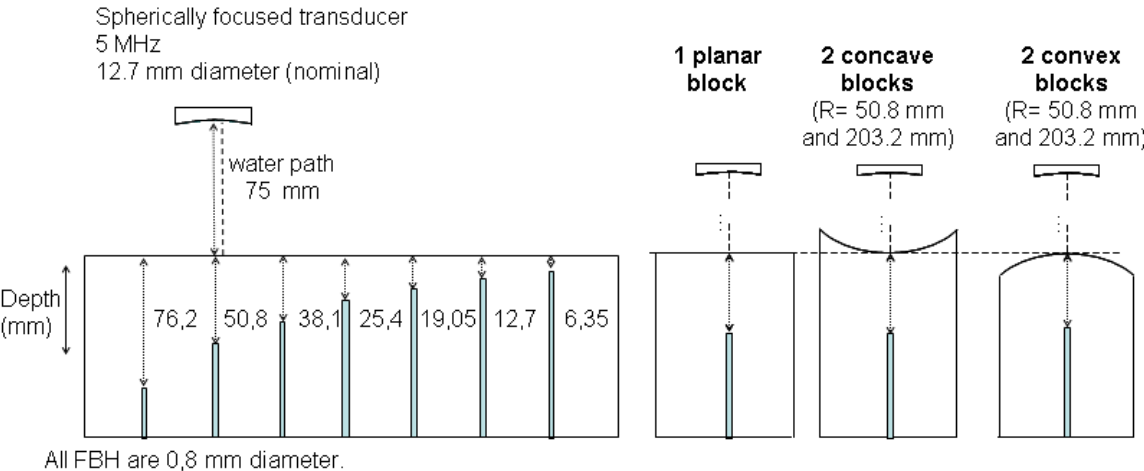


**FIGURE 1.** Description of the first study: surface curvature effect study.

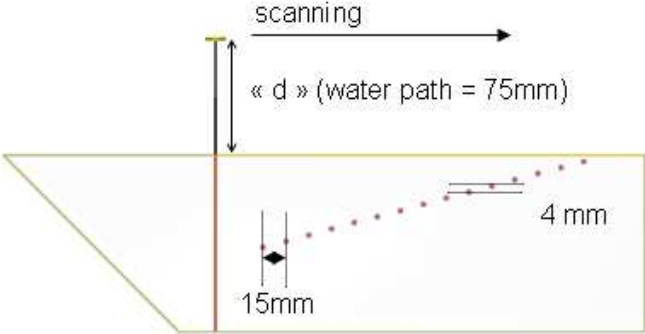


**FIGURE 2.** Description of second study: side drilled holes study.

## RESULTS

### Surface curvature effect study

#### Amplitudes of the response from flat-bottom holes

The echoes computations were performed with Civa release 9.2, in planar and cylindrical specimens. The following curves represent the amplitudes (dB) versus depths obtained for this study. The reference amplitude for all the echoes is the amplitude of the echo received from the 1/2 inch (12.7 mm) depth FBH under the planar surface.

For both the GPSS model and CIVA, the predictions are in good agreement with experimental measurements (Figure 3, 4 and 5), The differences between simulated and measured amplitudes are generally below 2 dB for both models.

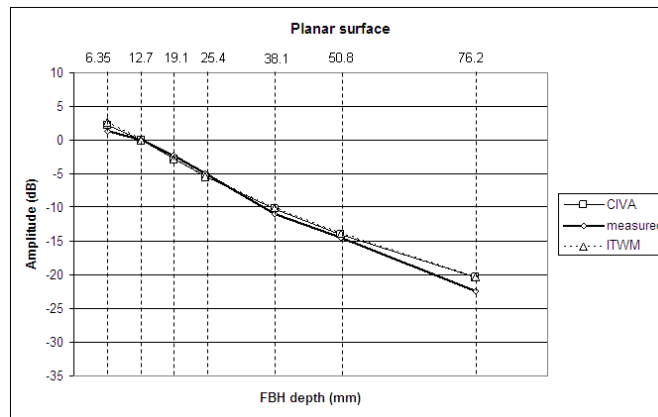


**FIGURE 3.** Experimental and simulated (GPSS and CIVA results) rectified longitudinal wave response amplitude of the flat-bottom hole at different depths and under a planar surface block. The reference amplitude for all the echoes is the amplitude of the echo received from the 1/2 inch (12.7 mm) depth FBH under the planar surface.

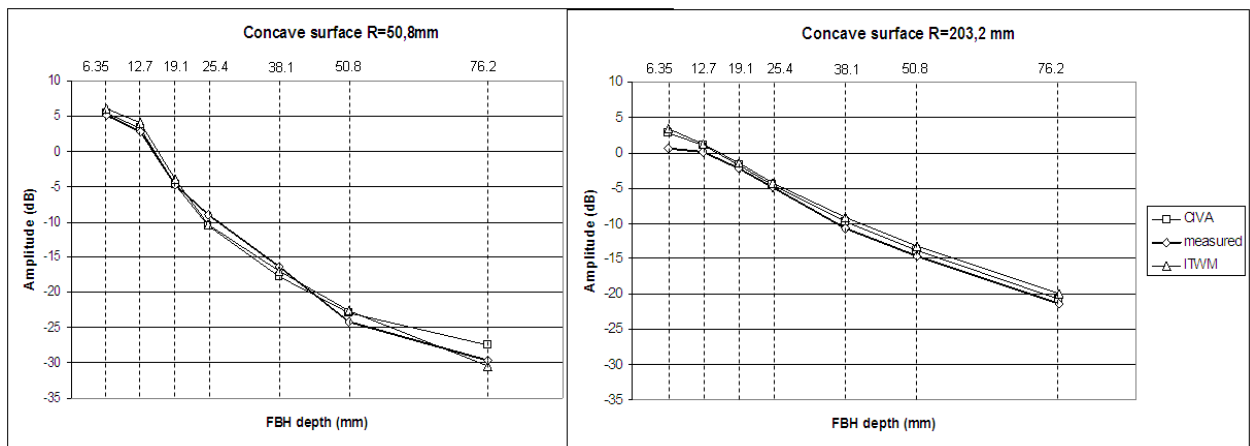


**FIGURE 4.** Experimental and simulated (GPSS and CIVA results) rectified longitudinal wave response amplitude of the flat-bottom hole at different depths and under concave surface blocks. The reference amplitude for all the echoes is the amplitude of the echo received from the 1/2 inch (12.7 mm) depth FBH under the planar surface.

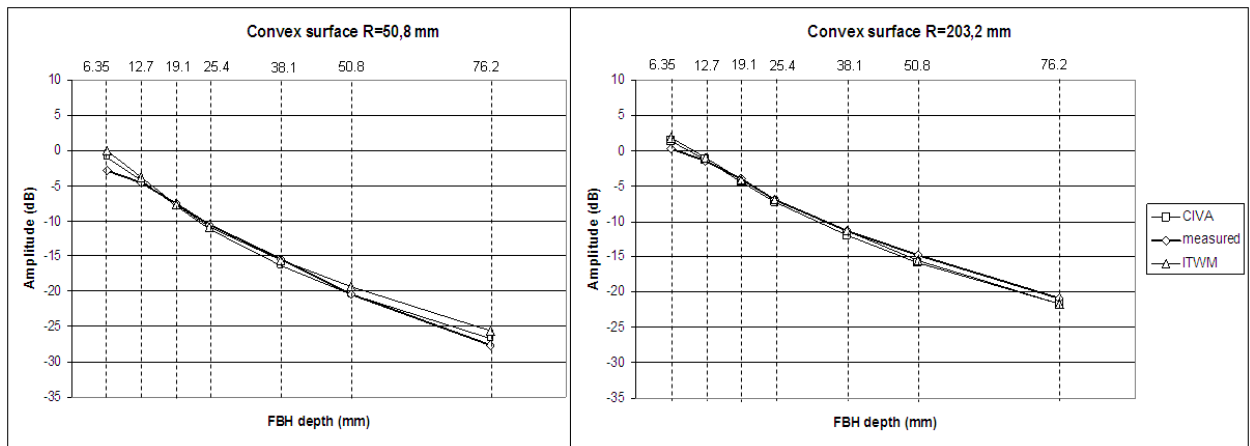


**FIGURE 5.** Experimental and simulated (GPSS and CIVA results) rectified longitudinal wave response amplitude of the flat-bottom hole at different depths and under convex surface blocks. The reference amplitude for all the echoes is the amplitude of the echo received from the 1/2 inch (12.7 mm) depth FBH under the planar surface.

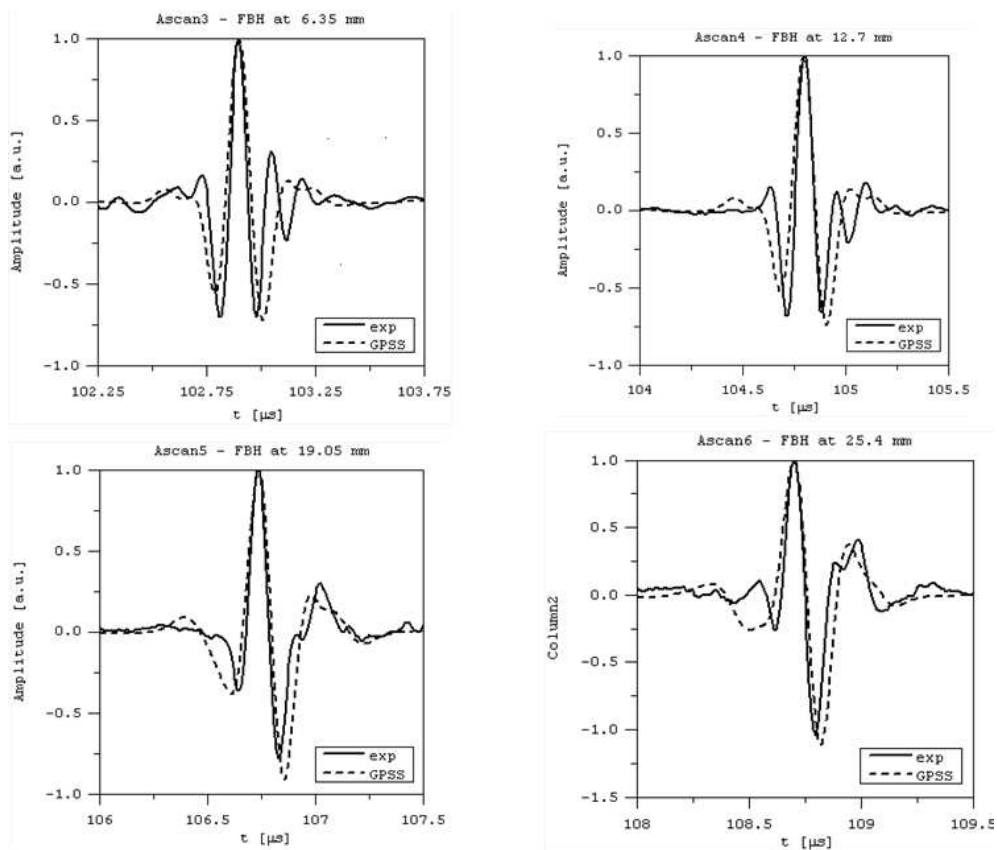


**FIGURE 6.** Comparison of experimental and simulated (GPSS code) waveform for flat bottomed holes at different depth (see figure) and under the concave surface (radius 50.8 mm).

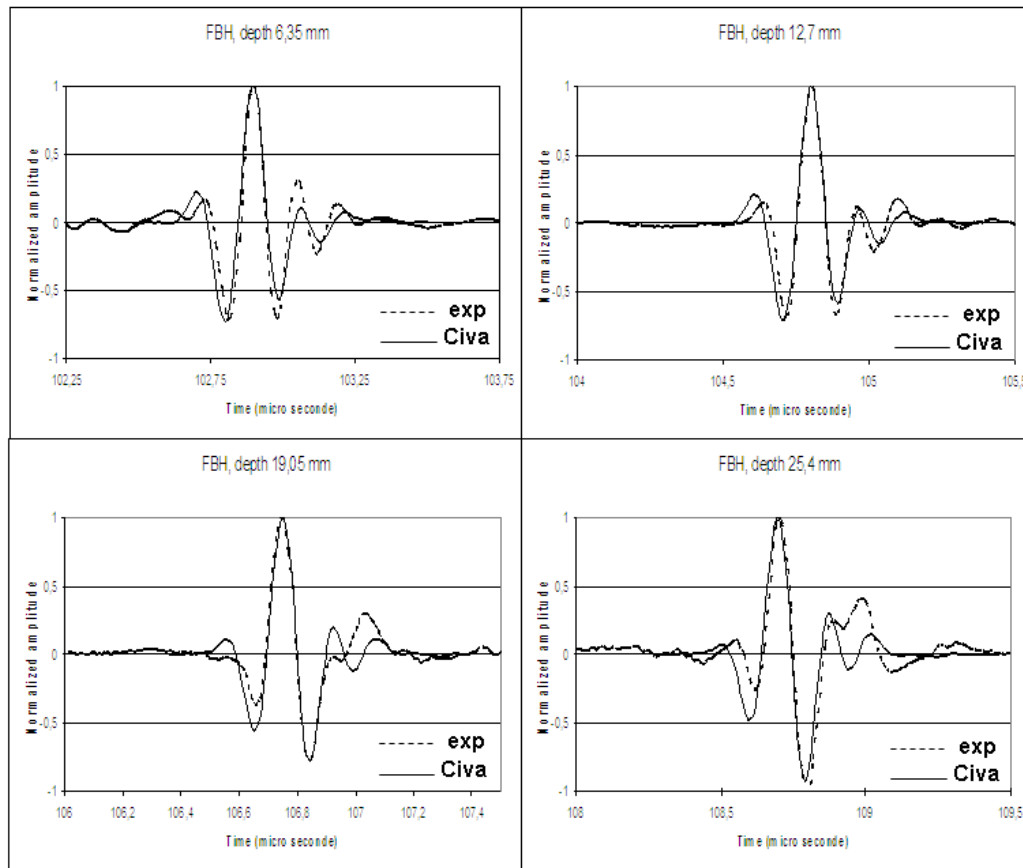


**FIGURE 7.** Comparison of experimental and simulated (CIVA) waveform for flat bottomed holes at different depth (see figure) and under the concave surface (radius 50.8 mm).

On the figures 3, 4 and 5 the effects (focusing or de-focusing) of the surface curvature are well observed for the FBH at the greatest depths: for these defects, with the planar, concave or convex surface with the 203.2 mm radius, the lowest amplitudes are around -20dB when they are around -25dB or -30dB for the concave and convex surface of small radius ( $R=50.8$  mm).

The simulated results obtained with both models are exactly the same for the planar and convex, radius 203 mm (figure 3 and 5) surfaces, but some differences occur for the other concave and convex surfaces (figures 4 and 5). The very good agreement between simulated and measured amplitudes for the planar interface indicates that the probe characteristics used for the simulation shall be relevant.

#### Waveform from flat-bottom holes

The waveforms of the echoes of 4 flat bottomed holes positioned under the concave surface (radius 50.8mm) are superposed on the figure 6 and 7. The shift of the echoes is well obtained with the 2 models. For both the GPSS model and CIVA, the simulated waveforms are in good agreement with the experimental one.

#### **Side-Drilled Holes (SDH) Longitudinal Waves Responses Study**

The simulation of SDH responses shows that the discrepancy increases with depth. As a very good agreement was obtained for the FBH responses over the planar specimen made of aluminum, we made another simulation with an attenuation law. The value for the attenuation was chosen so that the measured and simulated amplitudes of the SDH agree.

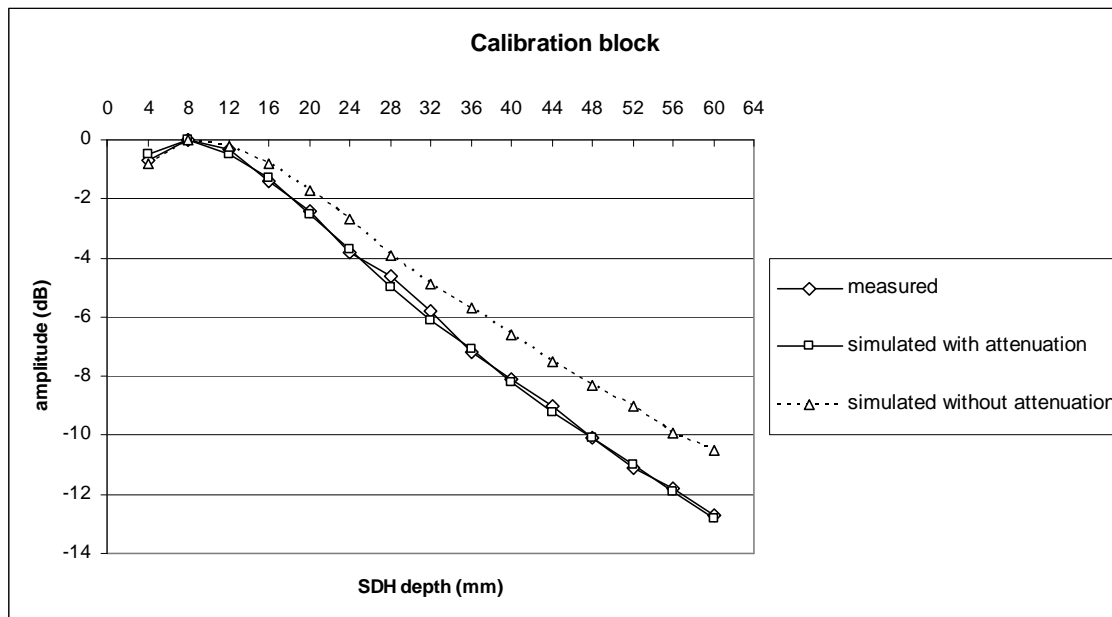


**FIGURE 8.** Experimental and simulated with and without attenuation (CIVA results) rectified longitudinal wave response amplitude of the side drilled holes at different depths. The reference amplitude for all the echoes is the amplitude of the echo received from side-drilled hole at a depth of 8 mm.

An exponential attenuation law was used:  $A_{att} = A e^{-\alpha \cdot d}$ ,  $d$  is the distance between the source and computation points,  $\alpha(f) = \alpha_0(f / f_0)^p$ . The wave attenuation is  $\alpha_0 = 0,03 \text{ dB} \cdot \text{mm}^{-1}$ , the power of the attenuation rate is  $p = 4$  for the wave frequency:  $f_0 = 5 \text{ MHz}$ .

The results are presented with and without attenuation (Figure 8), a very good agreement is obtained if the attenuation is used.

## CONCLUSION

The comparison between experiment and both codes (GPSS and CIVA) show a general good agreement for amplitudes and waveform echoes. The 2008 UT benchmark configurations were similar to those performed in 2007 for which all the participants observe the same discrepancy between simulation and measurement in the planar specimen. Using the probe provided and characterized by CNDE, the comparisons agree for different concave and convex mock-ups.

## REFERENCES

1. L. W. Schmerr, R. Huang, R. Raillon, S. Chatillon, S. Mahaut, S-J. Song, H-J. Kim, and M. Spies, "2007 ultrasonic benchmark studies of interface curvature – a summary," *Review of Progress in QNDE*, these proceedings (2008).
2. P. Calmon, S. Mahaut, S. Chatillon and R. Raillon, *Ultrasonics* **44**, E975 (2006).
3. M. Spies, "Modeling transient radiation of ultrasonic transducers in anisotropic materials including wave attenuation," in *Review of Progress in QNDE*, **21A**, edited by D. O. Thompson and D. E. Chimenti, AIP Conference Proceedings vol. 615, American Institute of Physics, Melville, NY (2002), pp. 807-814.
4. M. Spies, *J. Acoust. Soc. Am.* **110**, 68 (2001).

5. M. Spies, *J. Acoust. Soc. Am.* **107**, 2755 (2000).
6. B. A. Auld, *Wave Motion* **1**, 3 (1979).
7. N. Gengembre and A. Lhémy, *Ultrasonics* **38**, 495 (2000).
8. A. Lhémy, P. Calmon, I. Lecœur-Taïbi, R. Raillon and L. Paradis, *NDT&E Int.* **33**, 499 (2000).
9. R. Raillon, I. Lecœur-Taïbi, *Ultrasonics* **38** 527 (2000).
10. M. Darmon, S. Chatillon, S. Mahaut, L.J. Fradkin, A. Gautesen' "Simulation of a disoriented flaw in TOFDT configuration using GTD approach", *Review of Progress in QNDE*, these proceedings (2008).
11. 2008 Ultrasonic benchmarks, <http://www.wfndec.org/benchmarkproblemscurrent.htm>